# Rotating Fins in Phase Change Materials for Cyclable High-Power Density Latent Thermal Energy Storage.
# — Supplementary Information —

Biruk Agegnehu[a], Alessandro Ribezzo[a], Andrea Bottega[a], Matteo Morciano[a], Matteo Fasano[a] and Eliodoro Chiavazzo[a]

[a]*Department of Energy, Politecnico di Torino, Corso Duca degli Abruzzi 24, 10129 Torino, Italy*

ABSTRACT

This document includes supplementary Notes, tables, and pictures for the article *Rotating Fins in Phase Change Materials for Cyclable High-Power Density Latent Thermal Energy Storage*.

eliodoro.chiavazzo@polito.it (E. Chiavazzo)
ORCID(s):

# S1. Supplementary Note

## S1.1. Experimental Uncertainty and Error Analysis

To analyze the repeatability of the experiments and quantify the uncertainty associated with temperature measurements, each experimental condition was repeated three times. For each test, the temperatures measured by the four thermocouples were spatially averaged, and the uncertainty of the overall (spatially averaged) temperature was evaluated based on the standard deviation (SD) of these averaged values across repeated runs. This standard deviation is reported in Supplementary Table S1. Temperature measurements were obtained using K-type thermocouples (RS Components, model 787-7765), which have a manufacturer-specified uncertainty of $\pm 1.5$ °C. Regarding the uncertainty associated with image analysis, a quantitative error estimation is difficult to establish. As discussed in Ref. [51], determining the solid and liquid fractions relies on visual identification supported by image processing techniques. This procedure inherently involves subjective thresholding and interpretation, making a rigorous statistical uncertainty analysis challenging. Consequently, no explicit error bars are reported for the image-based measurements.

***Step 1: Test-number averaging*** : For each thermocouple and at each time instant, the temperature was averaged over the three repeated tests as

$$\overline{T}_{j,k} = \frac{1}{3} \sum_{r=1}^{3} T_{j,k}^{(r)} \tag{1}$$

***Step 2: Thermocouple averaging*** : The spatially averaged temperature at each time instant was obtained from the four thermocouples as

$$\overline{T}_{k} = \frac{1}{4} \sum_{j=1}^{4} \overline{T}_{j,k} \tag{2}$$

***Step 3: Standard deviation with respect to the thermocouple-averaged temperature*** : The standard deviation at each time instant was computed as

$$\sigma_k = \sqrt{\frac{1}{4-1} \sum_{j=1}^{4} \left( \overline{T}_{j,k} - \overline{T}_{k} \right)^2} \tag{3}$$

***Step 4: Mean standard deviation*** : The value reported in this study for the RotFinPCM (dynamic condition) corresponds to the mean standard deviation over the entire test duration. In contrast, for the static fin and baseline configurations, the reported uncertainty represents the maximum standard deviation observed among the thermocouples, calculated relative to each sensor's mean temperature.

$$\overline{\sigma} = \frac{1}{N} \sum_{k=1}^{N} \sigma_k \tag{4}$$

where $\overline{\sigma}$ the mean standard deviation and N is the number of recorded time samples.

## S1.2. Heat Loss Calculation

To quantify the heat transfer from the lateral walls of the PCM cylinder to the chamber, and its impact on the measured power density, we calculate the mean net heat flux across the lateral surface of the cylinder, considering the area exposed to heat transfer. The experiment was performed entirely inside a custom thermal chamber, heated by a hot air gun. The chamber air temperature was maintained at a setpoint of $T_\infty = 42,^\circ$ C using a thermostat with a hysteresis of $\pm 3,^\circ$ C, resulting in periodic modulation of the heat input. To minimize forced convection, the hot air gun outlet was equipped with a diffuser. Therefore, for the purpose of heat transfer estimation, the chamber air can reasonably be assumed to behave under natural convection conditions.

Local temperature measurements on the outer surface of the cylinder (Supplementary Figure S5) were used for the calculation. The periodic increase and decrease observed in surface temperature signal corresponds to the on–off cycling of the hot air gun. The PCM was contained within a hollow cylindrical resin shell with the following geometry:

**Geometry**

- Inner diameter: 40 mm
- Outer diameter: 56 mm
- Height: 50 mm

The chamber temperature was maintained at: $T_\infty = 42\,^\circ\text{C} \pm 3\,^\circ\text{C}$

**External Convection Resistance:** The external lateral surface area of the cylinder is:

$$A_{lat} = \pi D_o H = \pi \times 0.056 \times 0.05 \approx 0.0088\,\text{m}^2$$

Assuming a typical value for natural convection coefficient in air: $h = 8\,\text{W m}^{-2}\,\text{K}^{-1}$, The external convection resistance is therefore:

$$R_{\text{conv,out}} = \frac{1}{hA_{lat}} = 14.2\,\text{K/W} \tag{5}$$

The lateral heat power is:

$$Q_{\text{side}}(t) = \frac{T_{\text{cyl,out}}(t) - T_\infty(t)}{R_{\text{conv,out}}} \tag{6}$$

Since the hot air gun cycles symmetrically around 42 °C, the time-averaged ambient temperature can be approximated as $T_\infty = 42\,^\circ\text{C}$.

## Heat Loss Estimation

$$Q_{\text{side}}(t) = \frac{T_{\text{cyl,out}}(t) - T_\infty}{14.2} = \frac{\Delta T}{14.2}$$

From Supplementary Figure S5, the outer surface temperature ranges approximately as follows:

- Early stage: ∼ 45.4 °C (liquid sensible cooling, short duration)
- Middle stage: ∼ 43–44 °C (latent heat release, dominant stage of the experiment)
- Late stage: ∼ 40.5–41.5 °C (short final cooling stage)

Thus, $\Delta T = T_{\text{surface}} - 42$, where $T_{\text{surface}} = T_{\text{cyl,out}}$, which approximately ranges between:

- Maximum: +3.4 K
- Minimum: –1.5 K

When the surface temperature drops below 42 °C, heat is transferred from the chamber to the PCM. However, this condition occurs only briefly, since the chamber ambient temperature also decreases during the automatic on–off cycling of the hot air gun controlled by the thermostat.

### Representative Heat loss Values

$$Q_{\max} = \frac{3.4}{14.2} \approx 0.24 \text{ W}$$

When $\Delta T \approx 2$ K:

$$Q \approx 0.14 \text{ W}$$

When $\Delta T \approx 1$ K:

$$Q \approx 0.07 \text{ W}$$

The maximum lateral heat loss is approximately 0.24 W, but during most of the latent heat release stage, the typical lateral heat loss ranges between 0.07–0.14 W. This value is significantly lower than the mean power reported in Fig. 11. For example, compared to the rotating fin mean power of 4.8 W, a representative lateral heat loss of 0.1 W corresponds to $\frac{0.1}{4.8} \times 100 \approx 2\%$. Therefore, the lateral heat loss is negligible relative to the measured power output.

**Supplementary Table S1**
Summary of experimental measurement uncertainty for different experimental configurations

| Experimental configuration | Reference figure | $\Delta T$ (°C) | $\overline{\sigma}$ (°C) | Remark |
|---|---|---|---|---|
| Static fin configuration | Figure 7 | 20 | 2.32 | Maximum standard deviation |
| Baseline case | Figure 7 | 20 | 3.60 | Maximum standard deviation |
| RotFinPCM (dynamic condition) | Fig. 9A | 20 | 0.29 | Mean standard deviation |
| RotFinPCM (dynamic condition) | Fig. 9B | 10 | 0.54 | Mean standard deviation |
| Intermittent RotFinPCM (dynamic condition) | Fig. 10B | 20 | 0.30 | Mean standard deviation |

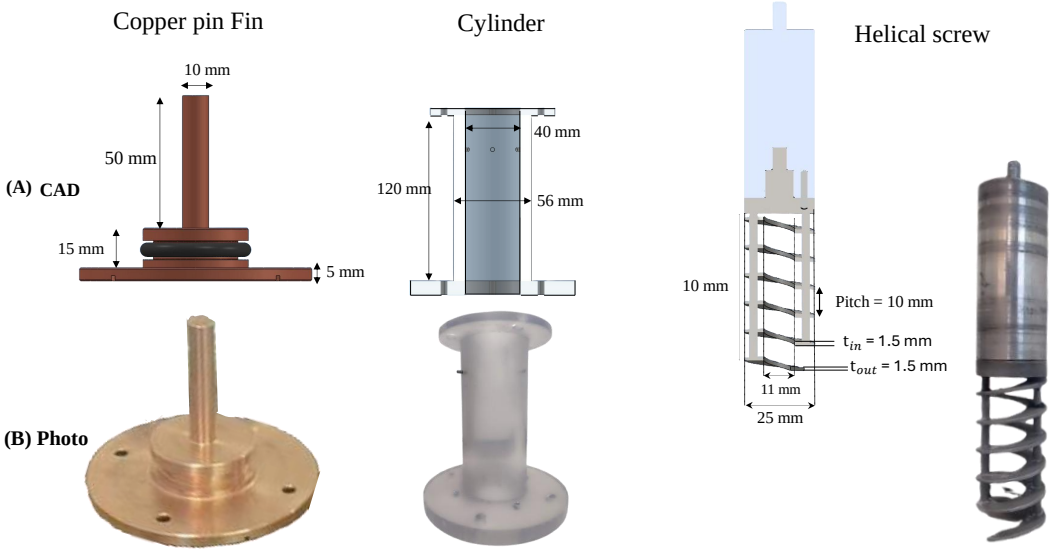


**Supplementary Figure S1: Geometrical dimensions of the experimental device components:** (A) CAD model and (B) photograph of the assembled setup.

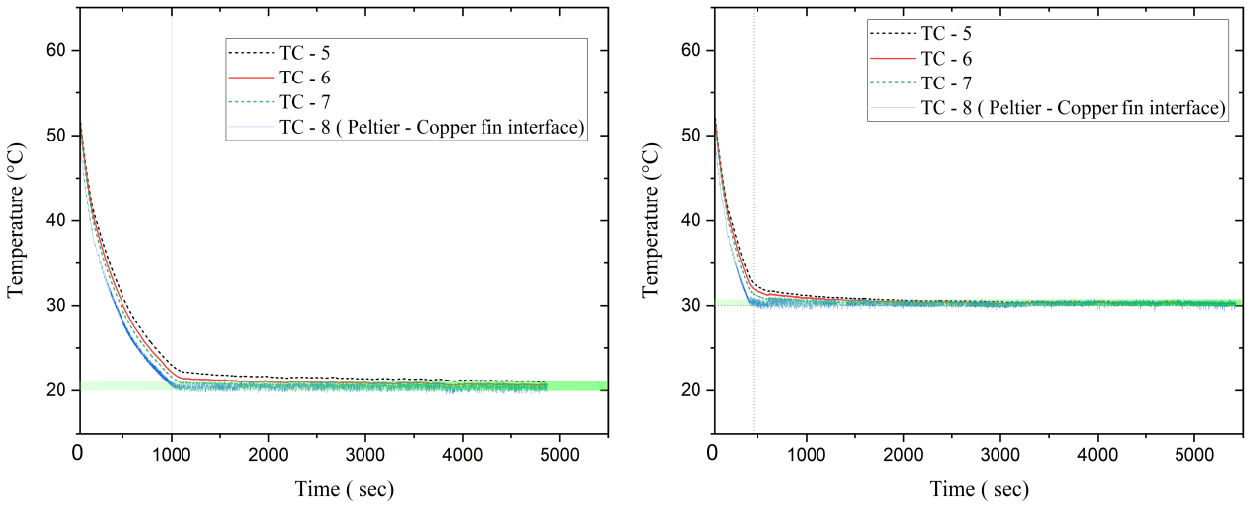


(a) $\Delta T = 20\,^{\circ}\mathrm{C}$. (b) $\Delta T = 10\,^{\circ}\mathrm{C}$.

**Supplementary Figure S2:** Temperature profile of the copper fin for (A) $\Delta T = 20\,^{\circ}\mathrm{C}$ and (B) $\Delta T = 10\,^{\circ}\mathrm{C}$. Where $\Delta T$ represents the temperature difference between the steady state copper fin and the Freezing temperature of the PCM ($T_f$). The initial stage of solidification shows a relatively short transient period during which the cooling fin temperature drops from its initial value to the predefined cooling temperature. Although this phase is brief, the profile is the same for both experimental conditions, and its effect on the performance analysis—based on the steady-state cooling temperature—is considered insignificant, as it occurs only in the initial stage and occupies a relatively short duration of the entire experiment.

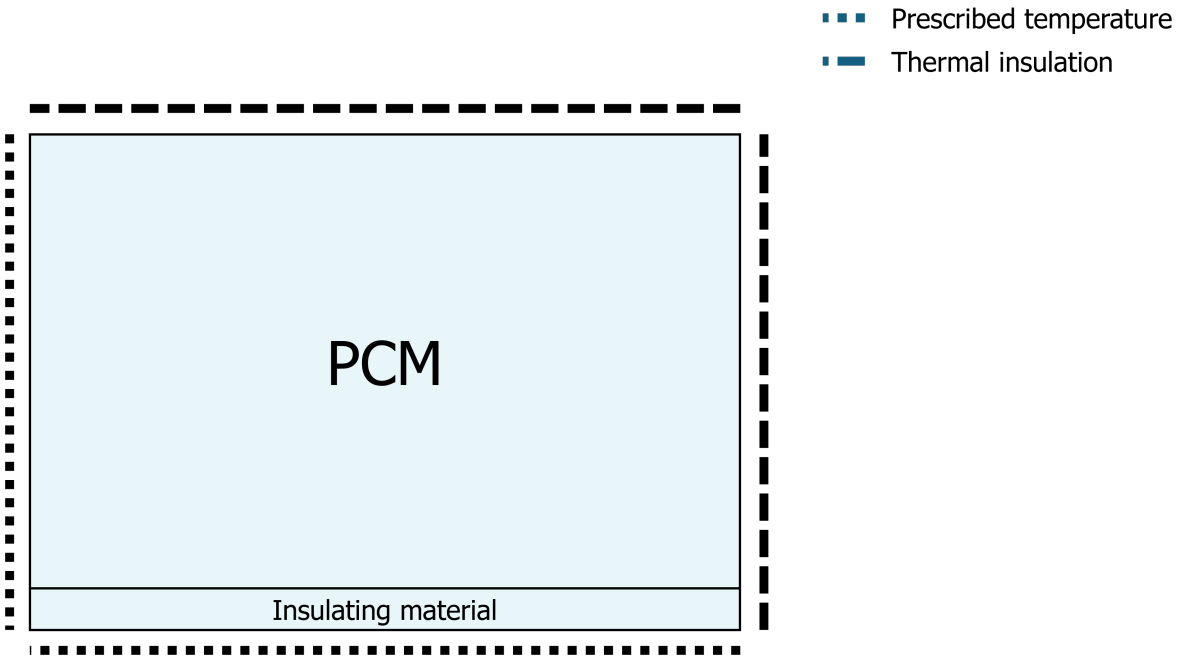


**Supplementary Figure S3:** Schematic of the boundary conditions applied to the CFD numerical models.

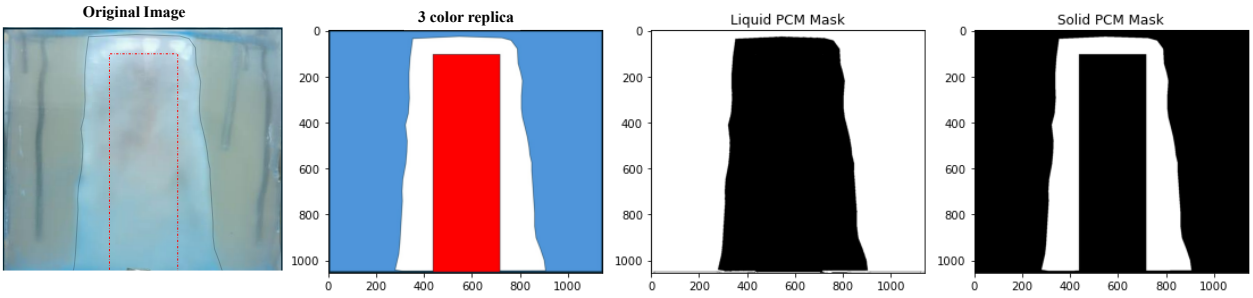


**Supplementary Figure S4:** Solid PCM fraction during solidification under $\Delta T = 10$ °C at time = 15 minutes after initiation of solidification, calculated from images using the Python-based OpenCV library

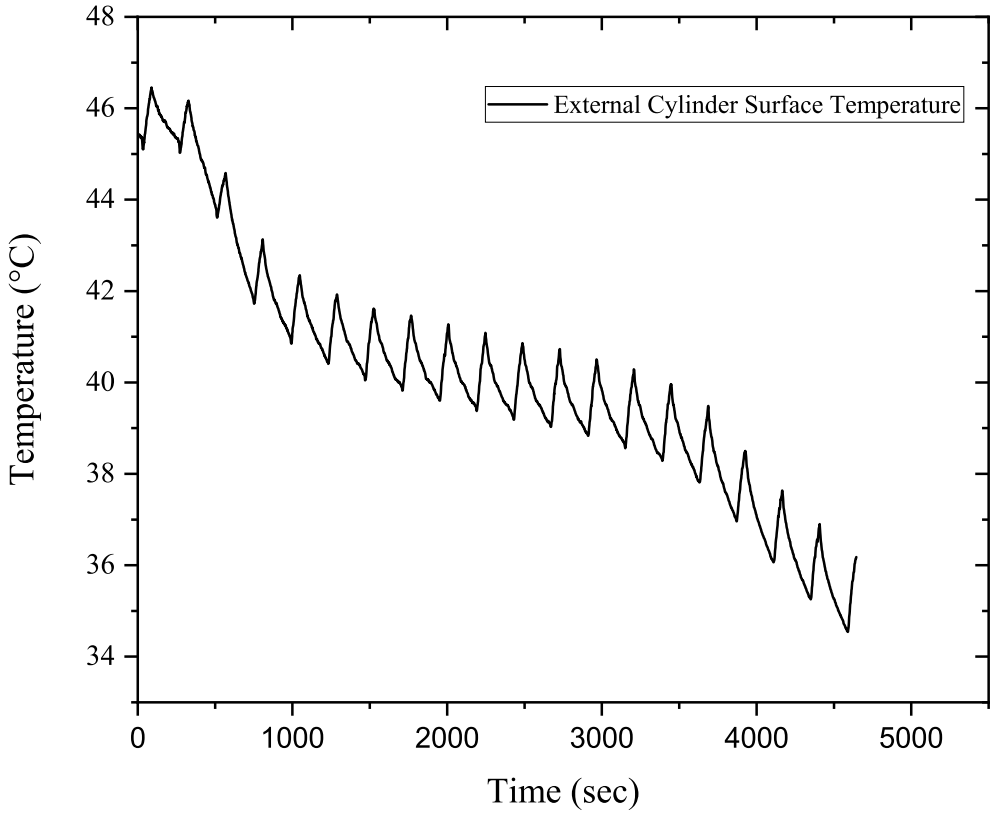


**Supplementary Figure S5:** Evolution of the external cylinder surface temperature during solidification under $\Delta T = 20\,^{\circ}\mathrm{C}$. The periodic rise and fall in the surface temperature are attributed to the on–off cycling of the hot air gun.